Response to reviewer #1

Thanks to the reviewer for your careful reading and your constructive comments and suggestions on our manuscript. The reviewer's comments and suggestions are shown as *italicized font*, our response to the comments is normal font. New or modified text is in normal font and in blue. Details are as follows.

Reviewer's comments:

Reviewer #1: *This work investigated the impact of low temperature on the formation of strong BrC chromophores in HULIS and proposed two mechanisms, one is that the low temperature may lead to a non-liquid phase state of ambient particles, potentially introducing kinetic limitation on the diffusion of reactive species from gas phase into the bulk aerosol and second low temperature promoted the reaction of phenols with NOx radicals while inhibited the atmospheric oxidation of nitrophenols, thus facilitating the accumulation of BrC chromophores such as nitrophenols in HULIS. Overall, the paper was well-organized, and the results are of broad interest. I would recommend the paper be accepted after revision, as outlined below.*

[Response]

Thanks for the reviewer's comments on this manuscript. Please check our point-by-point response and the modified text in the manuscript.

(1) line 48-50. Please elaborate further on the assertion that HULIS is under low-temperature conditions for the majority of its atmospheric lifetime. This statement serves as a critical foundation for the research motivation and requires more evidenced or references to support it.

[Response]

We sincerely appreciate the reviewer's insightful comment. In response, we now explicitly link the sharp decrease in ambient temperature during the vertical of transport of aerosols to the atmospheric evolution of HULIS. Furthermore, we have added key citations from (Heald et al., 2005; Liu et al., 2014; Pani et al., 2022; Textor et al., 2006; Wu et al., 2018), all of which provide observational support for the characteristic temperature regimes encountered by aerosols undergoing vertical and long-range transport, thus confirming the prolonged exposure of HULIS to low temperatures during its lifetime in the atmosphere. We believe this revised statement provides a much stronger and evidence-based foundation for the subsequent discussion on the need to understand low-temperature effects on HULIS properties and behavior.

[Revised]

Line 52-56: Once emits into or form in the atmosphere, vertical transport increased the altitude of HULIS-containing particles, leading to long-range transport (Chen et al., 2021; Slade et al., 2017). During vertical transportation, the ambient temperature sharply decreases, indicating that the atmospheric evolution of HULIS accompanies with low-temperature conditions during their majority lifetime (Heald et al., 2005; Liu et al., 2014; Pani et al., 2022; Textor et al., 2006; Wu et al., 2018).

(2) *line 83-84 and Text S1. This semi-quantification strategy was based on the experiment experience that substances with similar structures and equal concentrations yield comparable signal intensities in mass spectrometry. Please specify the criteria for selecting the semi-quantification proxy compounds. Additionally, a thorough discussion on the uncertainties associated with this semi-quantification approach should be provided.*

[Response]

We sincerely appreciate the reviewer's insightful comment. To address the concerns, we have added **Text S2** in the supporting information to clarify the criteria for selecting the semi-quantification proxy compounds and discuss the uncertainties of semi-quantitative strategy. Our selection of proxy compounds is guided by structural similarity to the target analytes, as ionization efficiency in mass spectrometry is dominantly determined by molecular structures – a principle illustrated in prior literature (Ma et al., 2022; Nozière et al., 2015). For instance, vanillin serves as surrogate standard for methoxy- and hydroxy- benzaldehydes; 1-t-butylimidazole quantifies imidazole derivatives; and 4-nitrophenol, 2,6-dimethyl-4-nitrophenol, and 4-methyl-5-nitrocatechol act as proxy compounds for the quantification of nitrophenols derivatives.

Text S2. Discussion on the uncertainty of semi-quantitative strategy

In atmospheric chemistry, the components of organic aerosols are always complex and no authentic standards can be used for quantification. In the analysis of these components, it has been widely suggested to use available proxy compounds for quantification (Ma et al., 2022; Nozière et al., 2015). For example, camphor-10-sulfonic acid is often used as surrogate standard for the quantification of α-pinene derivative organosulfates (Ma et al., 2022; Nguyen et al., 2014a). This strategy can achieve the quantitative analysis of various compounds in organic aerosols, but there are inevitable uncertainties which mainly come from the ionization efficiency difference between non-authentic standards and target analytes in mass spectrometric analysis (Nozière et al., 2015). Generally, the closer the molecular structures of surrogate standard is to the target analyte, the smaller the difference in ionization efficiency, resulting in the similar signal intensities in mass spectrometry.

Table S4 lists the deviation observed when different compounds were used as surrogate standards for quantification of each standard in this study. For instance, nitrophenol derivatives (4NP, 2N135T, and 4M5NC) showed quantification errors within 130% when used as surrogate standards for 26D4NP. Tetrahydroquinoline (1234THQ), an N-heterocyclic aromatic hydrocarbon, exhibited an error below 110% when quantifying 1tBI. However, even structurally similar surrogate standards may introduce an error of

a factor over 2. Both P3C and I2C belong to N-heterocyclic aromatic aldehydes, yet using I2C as a surrogate for P3C resulted in a 46% error. When the structurally distinct PAAE was used as a surrogate for P3C, the error reached 600%. Therefore, when adopting semi-quantitative strategies, it is critical to first identify the chemical structure of the target analyte and subsequently select surrogate standards with analogous structural features for quantification.

Regarding uncertainties, we provide an in-depth analysis supported by new validation data (Table S4). This table quantifies errors introduced when different proxy compounds are used for specific standards. For example, structurally close proxies (e.g., nitrophenol derivatives quantifying 26D4NP) typically yield errors below 130%, while even minor structural variations (e.g., I2C vs. P3C, both N-heterocyclic aromatic aldehydes) can cause ~46% deviation. This range aligns with the established uncertainty threshold (factor of ~2) reported for semi-quantitative methods in previous studies (Ma et al., 2022). We thus emphasize that while semi-quantification is essential for complex aerosol components lacking authentic standards, its accuracy is contingent on rigorous proxy selection.

[Revised]

Text S2. Discussion on the uncertainty of semi-quantitative strategy

In atmospheric chemistry, the components of organic aerosols are always complex and no authentic standards can be used for quantification. In the analysis of these components, it has been widely suggested to use available proxy compounds for quantification (Ma et al., 2022; Nozière et al., 2015). For example, camphor-10-sulfonic acid is often used as surrogate standard for the quantification of α-pinene derivative organosulfates (Ma et al., 2022; Nguyen et al., 2014a). This strategy can achieve the quantitative analysis of various compounds in organic aerosols, but there are inevitable uncertainties which mainly come from the ionization efficiency difference between non-authentic standards and target analytes in mass spectrometric analysis (Nozière et al., 2015). Generally, the closer the molecular structures of surrogate standard is to the target analyte, the smaller the difference in ionization efficiency, resulting in the similar signal intensities in mass spectrometry.

Table S4 lists the deviation observed when different compounds were used as surrogate standards for quantification of each standard in this study. For instance, nitrophenol derivatives (4NP, 2N135T, and 4M5NC) showed quantification errors within 130% when used as surrogate standards for 26D4NP. Tetrahydroquinoline (1234THQ), an N-heterocyclic aromatic hydrocarbon, exhibited an error below 110% when quantifying 1tBI. However, even structurally similar surrogate standards may introduce an error of a factor over 2. Both P3C and I2C belong to N-heterocyclic aromatic aldehydes, yet using I2C as a surrogate for P3C resulted in a 46% error. When the structurally distinct PAAE was used as a surrogate for P3C, the error reached 600%. Therefore, when adopting semi-quantitative strategies, it is critical to first identify the chemical structure of the target analyte and subsequently select surrogate standards with analogous structural features for quantification.

Table S4. The deviations observed when different compounds were used as surrogate standards for quantifying each target analyte

Deviation %	E2OCA	ES	SA	F25DC	VAN	18NaPA	9FLU	910PheQ	2AF	2FA	1234THQ	1tBI	4NP
E2OCA	100.0	4.3	8.8	17.6	101.9	64.2	9.5	324.7	21.7	2.5	163.1	155.8	93.5
ES	2400.0	100.0	207.6	421.0	2446.7	1539.0	224.3	7799.2	519.1	57.3	3916.1	3741.7	3014.4
SA	1164.8	47.8	100.0	203.7	1187.5	746.6	108.1	3787.0	251.3	27.0	1901.1	1816.4	1018.8
F25DC	570.7	23.7	49.2	100.0	581.8	365.9	53.2	1854.7	123.3	13.5	931.2	889.7	625.2
VAN	98.1	4.8	9.1	17.8	100.0	63.2	9.8	317.2	21.8	3.0	159.6	152.6	125.5
18NaPA	155.5	7.3	14.2	27.9	158.5	100.0	15.3	503.5	34.3	4.5	253.2	242.0	51.2
9FLU	1079.1	44.1	92.5	188.5	1100.1	691.6	100.0	3508.8	232.7	24.9	1761.4	1682.8	785.6
910PheQ	30.3	0.6	2.0	4.7	30.9	19.2	2.2	100.0	6.0	0.1	49.9	47.6	28.5
2AF	463.1	19.1	39.9	81.1	472.1	296.9	43.1	1505.4	100.0	10.9	755.8	722.1	409.9
2FA	4219.8	175.1	364.2	739.6	4301.9	2705.6	393.7	13714.5	912.1	100.0	6885.9	6579.1	4191.6
1234THQ	61.2	2.2	5.0	10.5	62.4	39.1	5.4	199.5	13.0	1.1	100.0	95.5	60.7
1tBI	64.0	2.3	5.2	10.9	65.3	40.9	5.6	208.9	13.5	1.2	104.7	100.0	60.9
4NP	106.9	3.3	9.8	16.0	79.7	195.5	12.7	351.1	24.4	2.4	164.7	164.2	100.0
2N135T	103.7	3.2	9.5	15.5	77.3	186.1	12.3	339.9	23.7	2.3	159.6	159.1	97.0
26D4NP	91.1	3.8	7.9	16.0	92.9	58.4	8.5	296.1	19.7	2.2	148.7	142.1	86.3
4M5NC	110.6	4.4	9.4	19.3	112.7	70.9	10.2	359.8	23.8	2.5	180.6	172.5	123.6
4NA	131.5	5.5	11.4	23.1	134.1	84.3	12.3	427.5	28.4	3.1	214.6	205.1	184.7
3NSA	2423.3	100.5	209.1	424.7	2470.4	1553.7	226.0	7875.9	523.8	57.4	3954.4	3778.2	5453.3
P3C	91.3	4.0	8.1	16.2	93.0	58.6	8.7	296.1	19.9	2.4	148.8	142.2	92.6
I2C	200.5	8.3	17.3	35.1	204.4	128.5	18.7	651.6	43.3	4.7	327.1	312.6	209.9
3PAAE	15.4	0.8	1.4	2.8	15.7	9.9	1.5	49.6	3.4	0.5	25.0	23.9	14.1
2AP	132.3	5.5	11.4	23.2	134.9	84.8	12.3	430.1	28.6	3.1	215.9	206.3	210.9
4MSPAA	139.6	6.0	12.3	24.7	142.3	89.6	13.3	453.2	30.4	3.6	227.7	217.6	163.9
4A5M2MBSA	1347.0	55.3	115.7	235.6	1373.2	863.5	125.1	4379.3	290.7	31.3	2198.5	2100.5	1400.4
3M4P1SA	763.1	31.3	65.5	133.4	778.0	489.1	70.8	2481.0	164.6	17.7	1245.5	1190.0	1021.5

Continue

Deviation %	2N135T	26D4NP	4M5NC	4NA	3NSA	P3C	I2C	3PAAE	2AP	4MSPAA	4A5M2MBSA	3M4P1SA
E2OCA	96.4	109.7	90.4	76.1	4.3	109.6	50.0	654.7	75.6	71.6	7.6	13.3
ES	3108.7	2634.1	2170.5	1824.8	99.5	2630.1	1197.5	15728.3	1814.0	1717.7	179.6	315.9
SA	1050.7	1278.5	1053.3	885.5	47.5	1276.6	580.8	7637.8	880.2	833.4	86.4	152.6
F25DC	644.8	626.3	516.1	433.9	23.5	625.4	284.7	3740.5	431.3	408.4	42.6	75.0
VAN	129.4	107.6	88.8	74.8	4.7	107.4	49.3	639.0	74.3	70.4	8.0	13.5
18NaPA	53.7	170.6	140.7	118.4	7.2	170.3	78.0	1014.6	117.7	111.5	12.4	21.2
9FLU	810.2	1184.4	975.8	820.3	43.8	1182.7	537.9	7076.9	815.4	772.0	79.9	141.2
910PheQ	29.4	33.3	27.3	22.9	0.6	33.3	14.8	202.4	22.7	21.5	1.6	3.4
2AF	422.7	508.3	418.8	352.1	19.0	507.5	230.9	3036.0	350.0	331.4	34.5	60.8
2FA	4322.7	4631.4	3816.1	3208.3	174.2	4624.5	2105.0	27658.2	3189.2	3019.8	315.1	554.8
1234THQ	62.6	67.2	55.3	46.4	2.2	67.1	30.3	402.6	46.1	43.7	4.3	7.8
1tBI	62.8	70.3	57.8	48.6	2.3	70.2	31.7	421.6	48.3	45.7	4.4	8.1
4NP	103.1	115.8	80.9	54.2	1.8	108.0	47.6	708.2	47.4	61.0	7.1	9.8
2N135T	100.0	112.3	78.4	52.5	1.8	104.7	46.2	687.0	46.0	59.2	6.9	9.5
26D4NP	89.0	100.0	82.4	69.3	3.8	99.8	45.4	597.2	68.9	65.2	6.8	12.0
4M5NC	127.5	121.4	100.0	84.0	4.4	121.2	55.1	725.7	83.5	79.1	8.1	14.4
4NA	190.4	144.4	118.9	100.0	5.4	144.1	65.6	862.1	99.4	94.1	9.8	17.3
3NSA	5623.9	2659.7	2191.5	1842.4	100.0	2655.7	1208.8	15883.5	1831.5	1734.2	180.9	318.6
P3C	95.5	100.2	82.6	69.4	4.0	100.0	45.6	597.0	69.0	65.4	7.0	12.2
I2C	216.5	220.0	181.3	152.4	8.3	219.7	100.0	1314.0	151.5	143.5	15.0	26.4
3PAAE	14.6	16.9	13.9	11.7	0.8	16.8	7.7	100.0	11.6	11.0	1.3	2.1
2AP	217.5	145.2	119.7	100.6	5.4	145.0	66.0	867.4	100.0	94.7	9.9	17.4
4MSPAA	169.0	153.2	126.3	106.2	6.0	153.0	69.8	913.8	105.6	100.0	10.7	18.6
4A5M2MBSA	1444.2	1478.5	1218.1	1024.0	55.0	1476.3	671.6	8832.5	1017.9	963.8	100.0	176.6
3M4P1SA	1053.5	837.6	690.1	580.1	31.1	836.3	380.5	5003.8	576.6	546.0	56.6	100.0

(3) Move compound identification and quantification from SI to the main text and a discussion of semi-quantification errors, as suggested above, should be incorporated into the manuscript (either in the main text or the SI).

[Response]

We thank the reviewer for this constructive suggestion. In accordance with the recommendation, compound identification and quantification originally in the supporting information (**Text S1**) have now been moved to Section 2.2 of the main text.

[Revised]

Line 104-120: The obtained data analysis was performed with the Compound Discoverer 3.3 software to generate reasonable molecular formulas and match fine structures to MS/MS data. The numbers of atoms restriction of formula were 1-40 for C, 1-100 for H, 0-40 for O, 0-6 for N, and 0-2 for S, with $0.3 \leq H/C \leq 3.0$, $0 \leq O/C \leq 1.2$, $0 \leq N/C \leq 1.0$, and $0 \leq S/C \leq 0.8$ (Kind and Fiehn, 2007). All of the mathematically formulas for each peak were performed with a mass tolerance of ± 5 ppm and peak areas more than three times of the blank sample. Three curated spectral databases, mzcloud library database, ChemSpider library database, and CFM-ID (https://cfmid.wishartlab.com) were applied to screen suspect candidates of structure (Allen et al., 2015). According to the Schymanski's confidence level (CL), these candidates were divided into confirmed structures (CL1), probable structures (CL2), and tentative candidates (CL3) (Schymanski et al., 2014). We showed two examples to illustrate the derivation processes of candidates in **Figure S6**.

A semi-quantitative strategy was conducted as follows: target analytes were quantified using external standard solutions of structurally analogous surrogate compounds (Nguyen et al., 2014b; Nozière et al., 2015). A representative application involved utilizing the standard curve of 4-methyl-5-nitrocatechol to simultaneously quantify three structural analogs: 4-methyl-5-nitrocatechol, 3-methyl-5-nitrocatechol, and 3,4-dimethyl-5-nitrocatechol. While this strategy enables quantification of compounds without commercially available standards, it introduces inherent uncertainties due to ionization efficiency variations between surrogates and target analytes (discussed in **Text S2**).

(4) Section 3.2. In the discussion on the potential sources of HULIS, the authors selected two PM haze events instead of high HULIS episodes. What's HULIS concentration during these two PM pollution events. Additionally, please include the mass spectra of HULIS samples from non-haze days for comparison with those in Event I and II. This would clarify whether the identified sources were specific to HULIS or more generally associated with $PM_{2.5}$.

[Response]

We appreciate the reviewer's insightful suggestions for strengthening our source analysis. In response, we have now integrated the requested data into Section 3.2. First, the HULIS-C concentrations during both haze events are explicitly stated: 6.68 μgC m^{-3} for Event I and 4.65 μgC m^{-3} for Event II, confirming the elevated HULIS loading of two haze events (2-3 times of the average value in non-haze

period, $PM_{2.5}$ concentration < 75 μg m^{-3}). Second, we have added comparative mass spectra of representative clean-day sample in Figure 2C. This comparison demonstrates that the majority of identified compounds are inherent to regional HULIS, while the concentrations of 9-fluorenone, nitrophenols, and other species emitted from coal combustion and biomass burning in the clean-day sample were significantly reduced. These revisions support our conclusion that coal combustion and biomass burning are important sources of HULIS in Northeast China, winter.

[Revised]

Line 169-177: To investigate drivers of the high concentrations and variable light absorption efficiency of HULIS in this study, we selected two samples (Event I and II) among all haze events ($PM_{2.5}$ concentration > 75 μg m^{-3}) that exhibited the maximal divergence in MAE_{365} values. Event I had higher $PM_{2.5}$ (159.6 ± 53.8 μg m^{-3}) and HULIS-C (6.68 μgC m^{-3}) but lower $MAE_{365,HULIS}$ (1.56 m^2 gC^{-1}), while Even II had lower $PM_{2.5}$ (83.7 ± 36.4 μg m^{-3}) and HULIS-C (4.65 μgC m^{-3}) but higher $MAE_{365,HULIS}$ (2.06 m^2 gC^{-1}). These contrasting events were chosen for potential sources comparison from the perspective of molecular composition. Considering the lowest $PM_{2.5}$ and HULIS-C concentration, the sample on January 13 ($PM_{2.5}$ = 14.1 ± 11.9 μg m^{-3}, HULIS-C = 0.97 μgC m^{-3}, $MAE_{365,HULIS}$ = 1.28 m^2 gC^{-1}) was selected to represent clean days. **Figure 2** exhibited the reconstructed MS spectra, the number, and concentration fraction of HULIS in both positive and negative modes.

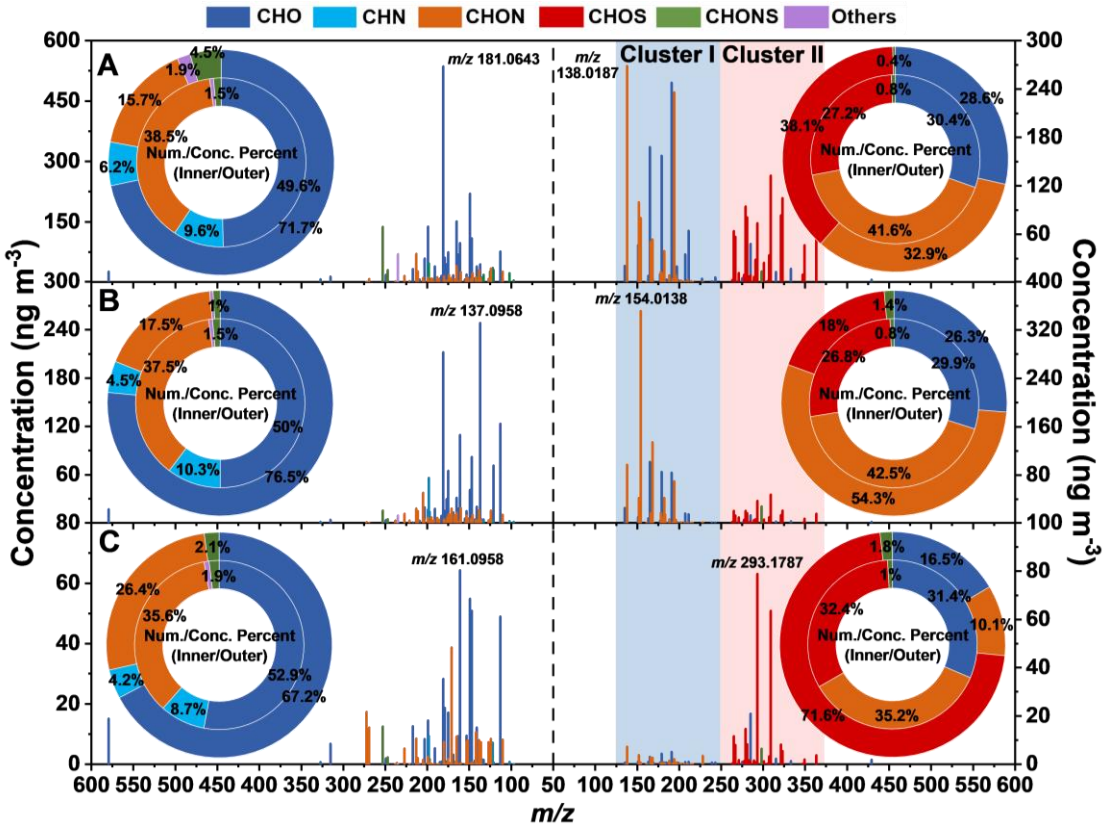

Figure 2. Reconstructed mass spectra of identified HULIS compounds during Event I (A), Event II (B), and Background (C). Spectra are shown for positive ionization mode (left panels) and negative ionization mode (right panels). m/z values increase from middle to both sides in all spectra. The most abundant ions are labeled with their m/z values. The accompanying pie charts represent the molecular class distribution

of the identified compounds: the inner/outer ring shows the relative abundance based on number/concentration of compounds.

(5) *Section 3.3. The discussion of the effect of temperature on BrC chromophore formation is arguably the most important aspect of this study. As the author proposed, low temperature promoted the exothermic process (e.g., reaction of phenols with NOx radicals) and hindered the endothermic chemical reactions (e.g., atmospheric oxidation of nitrophenols), thus facilitating the accumulation of BrC chromophores in HULIS. In addition to this qualitative thermodynamic explanation, a more in-depth discussion is encouraged. Specifically, how does low temperature alter the overall atmospheric chemistry and also any comparable results/findings/ mechanistic insights from previous literature that support your conclusions.*

[Response]

We deeply appreciate the reviewer's recognition of this study's core contribution and call for deeper mechanistic insights. While systematic experimental data on BrC evolution under low temperature remain limited, we have enhanced the discussion from the perspective of particle-phase retention mechanism and field observation evidence. Specifically, low temperature suppresses volatilization and enhances particle-phase retention of semi-volatile chromophores (He et al., 2006; Huang et al., 2006), providing a physicochemical pathway for BrC accumulation. This is directly corroborated by field observations of elevated nitroaromatic compound abundance in winter aerosols (Cai et al., 2022; Teich et al., 2017; Zhang et al., 2024), with researchers specifically linking such enhancement to "lower ambient temperatures in winter" (Cai et al., 2022; Zhang et al., 2024). These additions bridge our thermodynamic framework with empirical evidence, demonstrating how temperature alters atmospheric chemistry through both molecular stabilization and inhibition of degradation pathways. The mechanistic understanding of cold-region BrC chemistry requires more systematic experimental simulations to verify.

[Revised]

Line 247-260: Secondly, the formation of BrC chromophores was also important for the MAE_{365} enhancement of HULIS. On the one hand, the secondary formation of nitrophenols has been conclusively attributed to reaction of phenols with NO_x radicals (Bolzacchini et al., 2001; Finewax et al., 2018; Kroflič et al., 2021; Mayorga et al., 2021), a process that has been characterized as exothermic (Bolzacchini et al., 2001; Domingo et al., 2021). On the other hand, we have demonstrated that further atmospheric oxidation of nitrophenols proceeds via a ring-opening mechanism of benzene moiety (Qiu et al., 2024), which constitutes an endothermic reaction (Cao et al., 2021; Hems and Abbatt, 2018; Wang et al., 2017). From a thermodynamic perspective, low temperature not only promotes exothermic formation of nitrophenols while simultaneously suppressing their endothermic degradation via ring-opening. Furthermore, low temperature inhibits the volatilization and enhances the particle-phase retention of these volatile chromophores (He et al., 2006; Huang et al., 2006). This combined effect of low temperature led to the accumulation of strong BrC chromophores like nitrophenols within HULIS. This mechanism is consistent with field observations of enhanced nitroaromatic abundance in winter aerosols (Cai et al., 2022; Teich et al., 2017; Zhang et al., 2024). As such, we infer that ambient temperature plays

a critical role in promoting the transformation and light absorption of BrC chromophores, particularly in cold or/and high-altitude regions.

Reference

Allen, F., Greiner, R., and Wishart, D.: Competitive fragmentation modeling of ESI-MS/MS spectra for putative metabolite identification, Metabolomics, 11, 98–110, https://doi.org/10.1007/S11306-014-0676-4, 2015.

Bolzacchini, E., Bruschi, M., Hjorth, J., Meinardi, S., Orlandi, M., Rindone, B., and Rosenbohm, E.: Gas-phase reaction of phenol with NO3, Environ Sci Technol, 35, 1791–1797, https://doi.org/10.1021/ES001290M, 2001.

Cai, D., Wang, X., George, C., Cheng, T., Herrmann, H., Li, X., and Chen, J.: Formation of Secondary Nitroaromatic Compounds in Polluted Urban Environments, Journal of Geophysical Research: Atmospheres, 127, e2021JD036167, https://doi.org/10.1029/2021JD036167, 2022.

Cao, T. ting, Xu, T. fu, Deng, F. xia, Qiao, W. wei, and Cui, C. wei: Reactivity and mechanism between OH and phenolic pollutants: Efficiency and DFT calculation, J Photochem Photobiol A Chem, 407, 113025, https://doi.org/10.1016/J.JPHOTOCHEM.2020.113025, 2021.

Chen, J., Wu, Z. J., Zhao, X., Wang, Y. J., Chen, J. C., Qiu, Y. T., Zong, T. M., Chen, H. X., Wang, B. B., Lin, P., Liu, W., Guo, S., Yao, M. S., Zeng, L. M., Wex, H., Liu, X., Hu, M., and Li, S. M.: Atmospheric Humic-Like Substances (HULIS) Act as Ice Active Entities, Geophys Res Lett, 48, e2021GL092443, https://doi.org/10.1029/2021GL092443, 2021.

Domingo, L. R., Seif, A., Mazarei, E., Zahedi, E., and Ahmadi, T. S.: Quasi-RRHO approximation and DFT study for understanding the mechanism and kinetics of nitration reaction of benzonitrile with nitronium ion, Comput Theor Chem, 1199, 113209, https://doi.org/10.1016/J.COMPTC.2021.113209, 2021.

Finewax, Z., De Gouw, J. A., and Ziemann, P. J.: Identification and Quantification of 4-Nitrocatechol Formed from OH and NO3 Radical-Initiated Reactions of Catechol in Air in the Presence of NOx: Implications for Secondary Organic Aerosol Formation from Biomass Burning, Environ Sci Technol, 52, 1981–1989, https://doi.org/10.1021/ACS.EST.7B05864, 2018.

He, L. Y., Hu, M., Huang, X. F., Zhang, Y. H., and Tang, X. Y.: Seasonal pollution characteristics of organic compounds in atmospheric fine particles in Beijing, Science of The Total Environment, 359, 167–176, https://doi.org/10.1016/J.SCITOTENV.2005.05.044, 2006.

Heald, C. L., Jacob, D. J., Park, R. J., Russell, L. M., Huebert, B. J., Seinfeld, J. H., Liao, H., and Weber, R. J.: A large organic aerosol source in the free troposphere missing from current models, Geophys Res Lett, 32, 1–4, https://doi.org/10.1029/2005GL023831, 2005.

Hems, R. F. and Abbatt, J. P. D.: Aqueous Phase Photo-oxidation of Brown Carbon Nitrophenols: Reaction Kinetics, Mechanism, and Evolution of Light Absorption, ACS Earth Space Chem, 2, 225–234, https://doi.org/10.1021/ACSEARTHSPACECHEM.7B00123, 2018.

Huang, X. F., He, L. Y., Hu, M., and Zhang, Y. H.: Annual variation of particulate organic compounds in PM2.5 in the urban atmosphere of Beijing, Atmos Environ, 40, 2449–2458, https://doi.org/10.1016/J.ATMOSENV.2005.12.039, 2006.

Kind, T. and Fiehn, O.: Seven Golden Rules for heuristic filtering of molecular formulas obtained by accurate mass spectrometry, BMC Bioinformatics, 8, https://doi.org/10.1186/1471-2105-8-105, 2007.

Kroflič, A., Anders, J., Drventić, I., Mettke, P., Böge, O., Mutzel, A., Kleffmann, J., and Herrmann, H.: Guaiacol Nitration in a Simulated Atmospheric Aerosol with an Emphasis on Atmospheric Nitrophenol Formation Mechanisms, ACS Earth Space Chem, 5, 1083–1093, https://doi.org/10.1021/ACSEARTHSPACECHEM.1C00014, 2021.

Liu, J., Scheuer, E., Dibb, J., Ziemba, L. D., Thornhill, K. L., Anderson, B. E., Wisthaler, A., Mikoviny,

T., Devi, J. J., Bergin, M., and Weber, R. J.: Brown carbon in the continental troposphere, Geophys Res Lett, 41, 2191–2195, https://doi.org/10.1002/2013GL058976, 2014.

Ma, J., Ungeheuer, F., Zheng, F., Du, W., Wang, Y., Cai, J., Zhou, Y., Yan, C., Liu, Y., Kulmala, M., Daellenbach, K. R., and Vogel, A. L.: Nontarget Screening Exhibits a Seasonal Cycle of PM2.5Organic Aerosol Composition in Beijing, Environ Sci Technol, 56, 7017–7028, https://doi.org/10.1021/acs.est.1c06905, 2022.

Mayorga, R. J., Zhao, Z., and Zhang, H.: Formation of secondary organic aerosol from nitrate radical oxidation of phenolic VOCs: Implications for nitration mechanisms and brown carbon formation, Atmos Environ, 244, 117910, https://doi.org/10.1016/J.ATMOSENV.2020.117910, 2021.

Nguyen, Q. T., Christensen, M. K., Cozzi, F., Zare, A., Hansen, A. M. K., Kristensen, K., Tulinius, T. E., Madsen, H. H., Christensen, J. H., Brandt, J., Massling, A., Nøjgaard, J. K., and Glasius, M.: Understanding the anthropogenic influence on formation of biogenic secondary organic aerosols in Denmark via analysis of organosulfates and related oxidation products, Atmos Chem Phys, 14, 8961–8981, https://doi.org/10.5194/ACP-14-8961-2014, 2014a.

Nguyen, Q. T., Christensen, M. K., Cozzi, F., Zare, A., Hansen, A. M. K., Kristensen, K., Tulinius, T. E., Madsen, H. H., Christensen, J. H., Brandt, J., Massling, A., Nøjgaard, J. K., and Glasius, M.: Understanding the anthropogenic influence on formation of biogenic secondary organic aerosols in Denmark via analysis of organosulfates and related oxidation products, Atmos Chem Phys, 14, 8961–8981, https://doi.org/10.5194/ACP-14-8961-2014, 2014b.

Nozière, B., Kalberer, M., Claeys, M., Allan, J., D'Anna, B., Decesari, S., Finessi, E., Glasius, M., Grgić, I., Hamilton, J. F., Hoffmann, T., Iinuma, Y., Jaoui, M., Kahnt, A., Kampf, C. J., Kourtchev, I., Maenhaut, W., Marsden, N., Saarikoski, S., Schnelle-Kreis, J., Surratt, J. D., Szidat, S., Szmigielski, R., and Wisthaler, A.: The Molecular Identification of Organic Compounds in the Atmosphere: State of the Art and Challenges, Chem Rev, 115, 3919–3983, https://doi.org/10.1021/CR5003485, 2015.

Pani, S. K., Lee, C. Te, Griffith, S. M., and Lin, N. H.: Humic-like substances (HULIS) in springtime aerosols at a high-altitude background station in the western North Pacific: Source attribution, abundance, and light-absorption, Science of The Total Environment, 809, 151180, https://doi.org/10.1016/J.SCITOTENV.2021.151180, 2022.

Qiu, Y., Qiu, T., Wu, Z., Liu, Y., Fang, W., Man, R., Liu, Y., Wang, J., Meng, X., Chen, J., Liang, D., Guo, S., and Hu, M.: Observational Evidence of Brown Carbon Photobleaching in Urban Atmosphere at Molecular Level, Environ Sci Technol Lett, https://doi.org/10.1021/ACS.ESTLETT.4C00647, 2024.

Schymanski, E. L., Jeon, J., Gulde, R., Fenner, K., Ruff, M., Singer, H. P., and Hollender, J.: Identifying small molecules via high resolution mass spectrometry: Communicating confidence, https://doi.org/10.1021/es5002105, 2014.

Slade, J. H., Shiraiwa, M., Arangio, A., Su, H., Pöschl, U., Wang, J., and Knopf, D. A.: Cloud droplet activation through oxidation of organic aerosol influenced by temperature and particle phase state, Geophys Res Lett, 44, 1583–1591, https://doi.org/10.1002/2016GL072424, 2017.

Teich, M., Van Pinxteren, D., Wang, M., Kecorius, S., Wang, Z., Müller, T., Močnik, G., and Herrmann, H.: Contributions of nitrated aromatic compounds to the light absorption of water-soluble and particulate brown carbon in different atmospheric environments in Germany and China, Atmos Chem Phys, 17, 1653–1672, https://doi.org/10.5194/ACP-17-1653-2017, 2017.

Textor, C., Schulz, M., Guibert, S., Kinne, S., Balkanski, Y., Bauer, S., Berntsen, T., Berglen, T., Boucher, O., Chin, M., Dentener, F., Diehl, T., Easter, R., Feichter, H., Fillmore, D., Ghan, S., Ginoux, P., Gong, S., Grini, A., Hendricks, J., Horowitz, L., Huang, P., Isaksen, I., Iversen, T., Kloster, S., Koch, D.,

Kirkevåg, A., Kristjansson, J. E., Krol, M., Lauer, A., Lamarque, J. F., Liu, X., Montanaro, V., Myhre, G., Penner, J., Pitari, G., Reddy, S., Seland, Stier, P., Takemura, T., and Tie, X.: Analysis and quantification of the diversities of aerosol life cycles within AeroCom, Atmos Chem Phys, 6, 1777–1813, https://doi.org/10.5194/ACP-6-1777-2006, 2006.

Wang, Z. M., Zheng, M., Xie, Y. B., Li, X. X., Zeng, M., Cao, H. Bin, and Guo, L.: Molecular dynamics simulation of ozonation of p-nitrophenol at room temperature with ReaxFF force field, Wuli Huaxue Xuebao/ Acta Physico - Chimica Sinica, 33, 1399–1410, https://doi.org/10.3866/PKU.WHXB201704132, 2017.

Wu, G., Wan, X., Gao, S., Fu, P., Yin, Y., Li, G., Zhang, G., Kang, S., Ram, K., and Cong, Z.: Humic-Like Substances (HULIS) in Aerosols of Central Tibetan Plateau (Nam Co, 4730 m asl): Abundance, Light Absorption Properties, and Sources, Environ Sci Technol, 52, 7203–7211, https://doi.org/10.1021/ACS.EST.8B01251, 2018.

Zhang, M., Cai, D., Lin, J., Liu, Z., Li, M., Wang, Y., and Chen, J.: Molecular characterization of atmospheric organic aerosols in typical megacities in China, NPJ Clim Atmos Sci, 7, 1–12, https://doi.org/10.1038/S41612-024-00784-1, 2024.